University of Zurich[UZH]

Zurich Open Repository and Archive
University of Zurich
University Library
Strickhofstrasse 39
CH-8057 Zurich
www.zora.uzh.ch

Year: 2024

Delineation of the healthy rabbit duodenum by immunohistochemistry - A short communication

Meier Bürgisser, Gabriella ; Heuberger, Dorothea M ; Giovanoli, Pietro ; Calcagni, Maurizio ; Buschmann, Johanna

DOI: https://doi.org/10.1016/j.acthis.2024.152136

Posted at the Zurich Open Repository and Archive, University of Zurich
ZORA URL: https://doi.org/10.5167/uzh-260742
Journal Article
Published Version

The following work is licensed under a Creative Commons: Attribution 4.0 International (CC BY 4.0) License.

Originally published at:
Meier Bürgisser, Gabriella; Heuberger, Dorothea M; Giovanoli, Pietro; Calcagni, Maurizio; Buschmann, Johanna (2024). Delineation of the healthy rabbit duodenum by immunohistochemistry - A short communication. Acta Histochemica, 126(2):152136.
DOI: https://doi.org/10.1016/j.acthis.2024.152136

Acta Histochemica 126 (2024) 152136

Contents lists available at ScienceDirect

Acta Histochemica

journal homepage: www.elsevier.com/locate/acthis

Delineation of the healthy rabbit duodenum by immunohistochemistry – A short communication

Gabriella Meier Bürgisser [a], Dorothea M. Heuberger [b], Pietro Giovanoli [a], Maurizio Calcagni [a], Johanna Buschmann [a,*]

[a] Division of Plastic Surgery and Hand Surgery, University Hospital Zurich, Sternwartstrasse 14, 8091 Zurich, Switzerland
[b] Institute of Intensive Care Medicine, University Hospital Zurich, Sternwartstrasse 14, 8091 Zurich, Switzerland

ARTICLE INFO

Keywords:
Cryosection
Antigen retrieval
Immunofluorescence
Brunner's glands
Lymph nodes

ABSTRACT

The duodenum acts as a vital organ that performs fundamental physiological functions like digestion and nutrient absorption. Situated in the lower abdomen, the duodenum is located between the stomach and the jejunum. Usually, the duodenum is divided into four anatomical portions. We here compare paraffin embedded and cryosections of the healthy rabbit duodenum for research purposes. This analysis evaluates the differential outcomes resulting from the application of these fixation methodologies in conjunction with immunohistochemical assays targeting extracellular matrix markers collagen I, collagen III, fibronectin, α-smooth muscle actin (α-SMA), and proliferation marker ki67 as well as inflammatory marker PAR-2. Subsequent recommendations are provided based on our findings. Furthermore, the advantage of an antigen retrieval step in immunohistochemical labelling of paraffin sections was demonstrated and confirmed with an isotype negative control. Basic classical histological stainings as HE, GT and elastin were also performed. Comparison of different stainings and labellings was performed in serial sections, showing that adjacent to the circular muscle of the duodenum, the connective tissue was composed of collagen I and fibronectin, while the artery and vein walls were predominantly α-SMA positive. Moreover, PAR-2 immunohistochemical staining was performed, where particularly a type of gland adjacent to Brunner's glands showed prominent PAR-2 positive areas, while the Brunner's glands themselves were PAR-2 negative. Proliferating ki67 positive cells facing the lumen were highly abundant in all kinds of glands except for the Brunner's glands. This effort serves to furnish the research community with reference imagery pertinent to scientists opting for the rabbit duodenum model. The diversity of staining techniques employed herein establishes a foundational repository of images, primed for comparative analysis against pathological conditions. Furthermore, these images hold the potential to illustrate inter-species variations. For instance, they can be juxtaposed against murine or rat intestinal tracts, or even offer insights into the human context.

1. Introduction

In the digestive system, the duodenum acts as a vital and important organ that performs fundamental physiological functions like digestion and nutrient absorption. The name of the duodenum comes from its length, because 12 fingers laid horizontally beside each other have approximately the length of the duodenum, i.e. 23 – 25 cm for humans (Hou et al., 2022). In the lower abdomen, the C-shaped duodenum is located between the stomach and the jejunum, next to the liver. Usually, the duodenum is divided into four anatomical portions. The first portion is the superior duodenum (duodenal bulb, D1), followed by the descending (D2), the horizontal (D3), and the ascending duodenum (D4), the latter being fixed by the ligament of Teitz (Seman et al., 2019).

In contrast to the mucous cells in the stomach, where they uniformly cover the stomach surface (Johansson et al., 2013), the duodenal epithelium presents different cell types. Nutrient absorption in the duodenum is performed by absorptive cells located at the duodenal surface epithelium (Flemström and Garner, 1984) that additionally contains goblet cells (Takahashi et al., 2022), mucosal cells that serve for nutrient digestion and mucosal absorption. Furthermore, duodenal glands are found in the submucosa located beneath the *muscularis mucosae*. Among these mucous glands, the Brunner's glands (Krause, 2000) are

* Correspondence to: University Hospital Zurich, ZKF, Division of Plastic Surgery and Hand Surgery, Sternwartstrasse 14, 8091 Zurich, Switzerland.
E-mail address: johanna.buschmann@usz.ch (J. Buschmann).

https://doi.org/10.1016/j.acthis.2024.152136
Received 14 December 2023; Received in revised form 25 January 2024; Accepted 25 January 2024
Available online 31 January 2024
0065-1281/© 2024 The Author(s). Published by Elsevier GmbH. This is an open access article under the CC BY license (http://creativecommons.org/licenses/by/4.0/).

functionally important as they secrete mucous of high pH to neutralize the acidic content coming from the stomach. Furthermore, the alkaline mucous secreted by the Brunner's glands lubricates the intestinal walls and activates intestinal proteolytic enzymes, such as enteropeptidase (Zheng et al., 2009). These glands are named after a Swiss physician, Dr. Johann Konrad Brunner who first described them in 1687.

The rabbit intestines are anatomically similar to the human gastrointestinal tract, particularly for the New Zealand White Rabbit (Amiry et al., 2019). For researchers focusing on the diseased state of the duodenum and using the pre-clinical rabbit model, for example for the determination of efficacy of novel drugs against Crohn's disease (Kimmins and Billingham, 2001) or examining potential recurrence of duodenal papilla carcinoma after pancreatico-duodenectomy (Yu et al., 2023), the histological und immunohistochemical analysis at the endpoint needs basic reference images that are seldom provided for different important ECM markers in serial section, not to mention inflammatory markers like PAR-2. Such images of the healthy rabbit duodenum may help and support preclinical research and can be compared to the diseased state.

In this technical note, we therefore present the anatomy of the healthy rabbit duodenum from a histological and immunohistochemical perspective. Starting with differential outcomes of formalin fixation versus cryo embedding for immunohistochemical labelling of collagen I and III as well as for fibronectin, α-SMA and ki67, we continue with a recommendation of an antigen retrieval step in case of paraffin sections and immunohistochemistry (IHC). After that, we turn the focus on specific structures, such as the Brunner's glands, the intestinal villi, the lamina *muscularis mucosae* and the serous membrane, respectively. Such structures are depicted in serial sections and stained for different important extracellular matrix markers, including elastin, and also for proliferative ki67, among others. Furthermore, PAR-2 IHC staining of the duodenum is shown in detail. Given that PAR-2 is expressed throughout the gastrointestinal tract, this inflammatory marker is interesting for the comparison in the normal healthy duodenum and potential diseased states (Kawabata et al., 2001).

In summary, we here provide representative images of the healthy rabbit duodenum for comparison to a diseased state using the New Zealand White Rabbit model for research purpose. Furthermore, these images hold the potential to illustrate inter-species variations. For instance, they can be juxtaposed against murine or rat duodenum, or even offer insights into the human context. Researchers may get interested and implement this pre-clinical animal model in their projects.

2. Materials and methods

2.1. Duodenum extraction

Rabbit duodenum was received from a dead female New Zealand White rabbit that was included in a calvarial bone defect project. This corresponding project was licensed by the Animal Ethics Committee at local authorities (Canton Zurich ZH 115/2015 and 090/2021) (Ghayor and Weber, 2018; Siegenthaler et al., 2020). The whole duodenum was used as received after isolation from this cadaver. Then, following storage on ice for 20 min and sectioning, it was ready for histology.

2.2. Histology and Immunohistochemistry

The duodenum pieces were cut in 2 parts for either paraffin embedding or cryo embedding. Paraffin embedding included fixation in formalin for one day, dehydration, paraffin-embedding and sectioning into 5-μm-thick slices. Before they were stained, paraffin embedded sections were deparaffinized utilizing xylene and rehydrated (decreasing gradient of ethanol).

As for the cryopreservation samples, they were embedded in Tissue-Tek® O.C.T. (Sakura, Alphen aan den Rijn, The Netherlands, Europe). Then, they were frozen before cryosections of 5 μm thickness were cut with a microtome. Subsequently, they were thawed and fixed with formalin for 10 min, and finally washed with 1xTBS, followed by IHC procedures. According to general protocols, Elastica van Gieson (EL), Masson Goldner Trichrome (GT) and Haematoxylin&Eosin (HE) stainings were performed. For IHC, an antigen retrieval (AR) step was performed for paraffin sections, using 10 mM citrate buffer (pH 6.0) with 0.05% Tween-20 for 20 min at 95 °C. In some cases, no AR was made in order to generate a control for the comparison of conditions with and without AR. For certain epitopes, such as ki67 and α-SMA, corresponding sections were permeabilized with 0.5% Triton X-100 in 1xTBS for 10 min, followed by three times washing with 1xTBS. After that, the sections were blocked in 5% donkey serum and 1% BSA in 1xTBS for 1 h (at room temperature (RT)). Next, sections were incubated with mouse monoclonal anti-collagen I antibody (ab90395; Abcam, Lucerne, Switzerland, 1:200 dilution) or mouse monoclonal anti-collagen III antibody (AF5810; Acris, Wettingen, Switzerland, 1:200 dilution) or mouse monoclonal anti-αSMA antibody (A2547; Sigma-Aldrich, Buchs, Switzerland, 1:500 dilution) or mouse monoclonal anti-fibronectin antibody (F0791; Sigma-Aldrich, Buchs, Switzerland, 1:200 dilution) or mouse monoclonal anti-ki67 antibody (NBP2–22112; Novus Biologicals, 1:500 dilution) or mouse monoclonal anti-PAR-2 antibody (Santa Cruz Biotechnology, sc-13504 (SAM11), 1:250 dilution) on Refine-kit (anti-Rabbit-Polymer) and histofine-Mouse Polymer (1:50 dilution) diluted in 3% BSA in 1xTBS overnight at 4 °C (Table 1).

Dilutions of antibodies were either taken from technical sheet data, provided by the suppliers or by titration of different concentrations and comparison of staining intensities. The laboratory validation of PAR-2 antibody had been performed before (Meier Bürgisser et al., 2020). In short, the validation consisted of denoting the *specificity* of PAR-2 antibody for rabbit brain tissue as well as the *reproducibility* of PAR-2 labelling, using rabbit Achilles tendon tissues after operation, stained at 3, 6 and 12 weeks, respectively, utilizing different lots of the antibody (Meier Bürgisser et al., 2020). Further information has been published earlier (Meier Bürgisser et al., 2020; Meier Bürgisser et al., 2021; Meier Bürgisser et al., 2022). Normal Mouse Serum Control (08–6599, Invitrogen, no dilution) was used; the corresponding sections were incubated with it (4 °C overnight) and used as a negative control for all antibodies.

Fluorescent IHC was performed for collagen I and III, fibronectin and α-SMA, respectively, and for a control also for ki67. Chromogenic IHC labelling was conducted for collagen I and III, fibronectin, ki67 and PAR-2, respectively, and for a control also for α-SMA. The supernatant primary antibody solution was removed and samples were then washed with 1xTBS for fluorescent IHC before incubation with the secondary donkey anti-mouse Alexa-488 antibody (A-21202; Invitrogen, Basel, Switzerland, 1:500 dilution) and 10 μg/mL 4'6-diamidino-2-phenylindole dilactate (DAPI) (Sigma-Aldrich, Switzerland) diluted in 3% BSA

Table 1
Antibodies and conditions for IHC labellings.

Primary antibody	*Supplier*	*Dilution*
Mouse monoclonal anti-collagen I	ab90395; Abcam, Lucerne, Switzerland	1:200
mouse monoclonal anti-collagen III	AF5810; Acris, Wettingen, Switzerland	1:200
Mouse monoclonal anti-αSMA	A2547; Sigma-Aldrich, Buchs, Switzerland	1:500
mouse monoclonal anti-fibronectin	F0791; Sigma-Aldrich, Buchs, Switzerland	1:200
mouse monoclonal anti-ki67	NBP2-22112; Novus Biologicals	1:500
mouse monoclonal anti-PAR-2	Santa Cruz Biotechnology, sc-13504 (SAM11) on Refine-kit (anti-Rabbit-Polymer) and histofine-Mouse Polymer	1:250 1:50
Normal Mouse Serum; Isotype Negative Control	08-6599, Invitrogen	no dilution

in 1xTBS for 1 h (RT). Finally, the slides were washed in 1xTBS and mounted, utilizing Dako Fluorescence Mounting Medium (Agilent, Basel, Switzerland).

For chromogenic IHC, samples were blocked with 3% hydrogen peroxide solution in water for 10 min (RT) and subsequently washed 3 times with 1xTBS. Primary antibody detection was made with a biotinylated anti-mouse IgG secondary antibody and streptavidin-horseradish peroxidase (HRP) (ZytoChem Plus HRP Kit Mouse; Zytomed Systems, Muttenz, Switzerland). Then, colorimetric detection was conducted according to the manufacturer's protocol with DAB (DAB Substrate Kit High Contrast; Zytomed Systems, Germany). Last, slides were given a wash in tap water and mounted, using Faramount Aqueous Mounting Medium from Agilent.

With a slide scanner (Pannoramic 250 Flash II, 3Dhistech, Budapest, Hungary), images of whole tissue sections were taken. We made snapshots of fields of view (FOVs) with CaseViewer-Sofware v.2.1 or imaged them with a Leica 6000 light microscope (Leica, Basel, Switzerland). The techniques and stainings used in this study are summarized in Table 2.

3. Results and discussion

3.1. Fixation of the tissue

Fixation of the tissue as a preparation for histological staining is sometimes a challenging choice for researchers after performing animal experiments. Cellular components have to be adequately preserved, autolysis and displacements of cell constituents, such as antigens and enzymes, have to be prevented and finally the tissue of interest has to be stabilized against the harmful mechanical effects of the subsequent processing (Ramos-Vara, 2005). Fixatives can be divided into two categories, cross-linking and coagulating fixatives, respectively. The gold standard cross-linking fixative is formalin, which binds to amino groups and reactive hydrogen atoms, resulting sometimes in adversely changing the conformation of macromolecules. This can harm the recognition of the proteins by antibodies, rendering immunohistochemistry almost impossible (complete loss of immunoreactivity). Nevertheless, formalin fixation with subsequent paraffin embedding is one of the most used cross-linking fixation techniques (Sadeghipour and Babaheidarian, 2019), although concerns about its toxicity, carcinogenicity and mutagenic effects led to the testing of alternatives, such as glyoxal acid free fixative (Ryska et al., 2023).

In contrast, coagulating fixatives like ethanol are used, which precipitates proteins by breaking hydrogen bonds, however without cross-linking the proteins. Disadvantages of this method are inadequate cellular preservation and a shift in intracellular immunoreactivity. Ethanol fixation has been reported to be much less reliable than formalin fixation, because ethanol fixation can lead to histological distortion, cell shrinkage and vacuolization (Prentø and Lyon, 1997). A further fixation technique is the cryopreservation, also called cryo embedding. Based on the freezing of freshly harvested tissue after embedding in Tissue-Tek®, cryo embedding has been reported to potentially lead to morphological changes in the tissue. Furthermore, the crystallized water may damage the tissue to some extent (Katoh, 2017). Any kind of fixation technique may inactivate enzymes to some degree, however, it can still allow proper morphological analysis (Fowler et al., 2008). Obviously, full denaturation should by all means be avoided (Tsutsumi, 2021).

Further fixation techniques have been reported, such as the Bouin solution, paraformaldehyde-lysine-periodate, or acetic formalin (Salguero et al., 2001). Moreover, antigen retrieval (AR) steps are used to retrieve the loss of antigenicity and to theoretically reach the state of proteins in their prefixation conformation. In addition, enzymatic AR and heat-induced epitope retrieval have been described with the help of a microwave oven, a pressure cooker or a steamer (Ramos-Vara, 2017). Permeabilisation chemicals allow access antigens inside cells, among them detergents like TritonX-100, Tween20, glycine, and hydrogen peroxide (Rosas-Arellano et al., 2016).

In this report on rabbit duodenum anatomy, we have compared formalin fixation with a buffered 4% formalin solution to cryo embedding. It was hypothesized that cryo embedding is superior to formalin fixation. During the comparison, it turned out that neither cryo embedding nor formalin fixation was always better. It highly depended on the immunohistochemical target structure and on the detection system (chromogenic versus fluorescent detection). Recommendations which specific fixation techniques has to be favoured will be given after the discussion of several antibodies and the comparison of paraffin sections versus cryosections.

Fig. 1 shows healthy rabbit duodenum sections and immunohistochemical labelling for collagen I, collagen III, fibronectin, ki67 and α-SMA, to compare paraffin section with cryosection. We chose DAB for the chromogenic detection system, because amino ethyl carbazole (AEC) has been reported to be worse (Hira et al., 2019), which we were able to confirm. Both, paraffin and cryo sections show the collagen I positive areas as dark brown areas with a light brown background, however, in cryo sections the contrast is more pronounced because the cells and the surrounding tissue appear rather bluish than brown, which demarcates to the dark brown collagen I in a well visible way.

Collagen I rich areas in the rabbit duodenum are particularly found at serous membrane, which can be nicely seen at the lowest magnifications for both, the paraffin and the cryosections, respectively (Fig. 1). Moreover, there is a collagen I rich zone in the glands, particularly around cells facing the lumen of the glands. At the highest magnification, these cells can be depicted quite well. As the collagen I intensity in the cryosections is slightly more pronounced than in the corresponding paraffin sections at the highest magnification, paraffin fixation may be favoured over cryo embedding, at least for these zoom-in situations.

As for the collagen III expression, only the serous membrane and the connective tissue between the longitudinal muscle and the inner part of

Table 2
Overview of markers, techniques and stainings used in this study. *Key:* ECM = Extracellular Matrix, Chro = Chromogenic detection, Fluo = Immunofluorescence, AR = antigen retrieval. Note that for Fibronectin and mouse isotype negative control (NC) images with and without AR-step are shown; "AR" and "no AR" is mentioned on these images and AR was only performed in paraffin sections. For all other stainings on paraffin sections there is no mention about AR, but AR was performed.

Marker	*Description/ Purpose*	*Fixation*	*AR*	*Detection System*
Collagen I (Col I)	Structural protein in ECM	Para + cryo	Yes	Chro + Fluo
Collagen III (Col III)	Structural protein in ECM	Para + cryo	Yes	Chro + Fluo
Fibronectin (Fn)	Glycoprotein for network building of the ECM	Para + cryo	Yes + No	Chro + Fluo
alpha smooth muscle actin (α-SMA)	Contractile smooth muscle fibres in ECM	Para + cryo	Yes	Fluo (+Chro)
ki67	Cell nucleus protein expressed in proliferating cells	Para + cryo	Yes	Chro (+Fluo)
PAR-2	Inflammation-related protein on cell surface	Para	Yes	Chro
Mouse isotype negative control (NC)	(Normal mouse serum)	Para	Yes + No	Chro + Fluo
Elastica van Gieson (EL)	Elastic fibers	Para	(classical histology)	(classical histology)
Masson Goldner Trichrome (GT)	Connective tissue structures	Para	(classical histology)	(classical histology)
HE	Most structures for comprehensive structural overview	Para	(classical histology)	(classical histology)

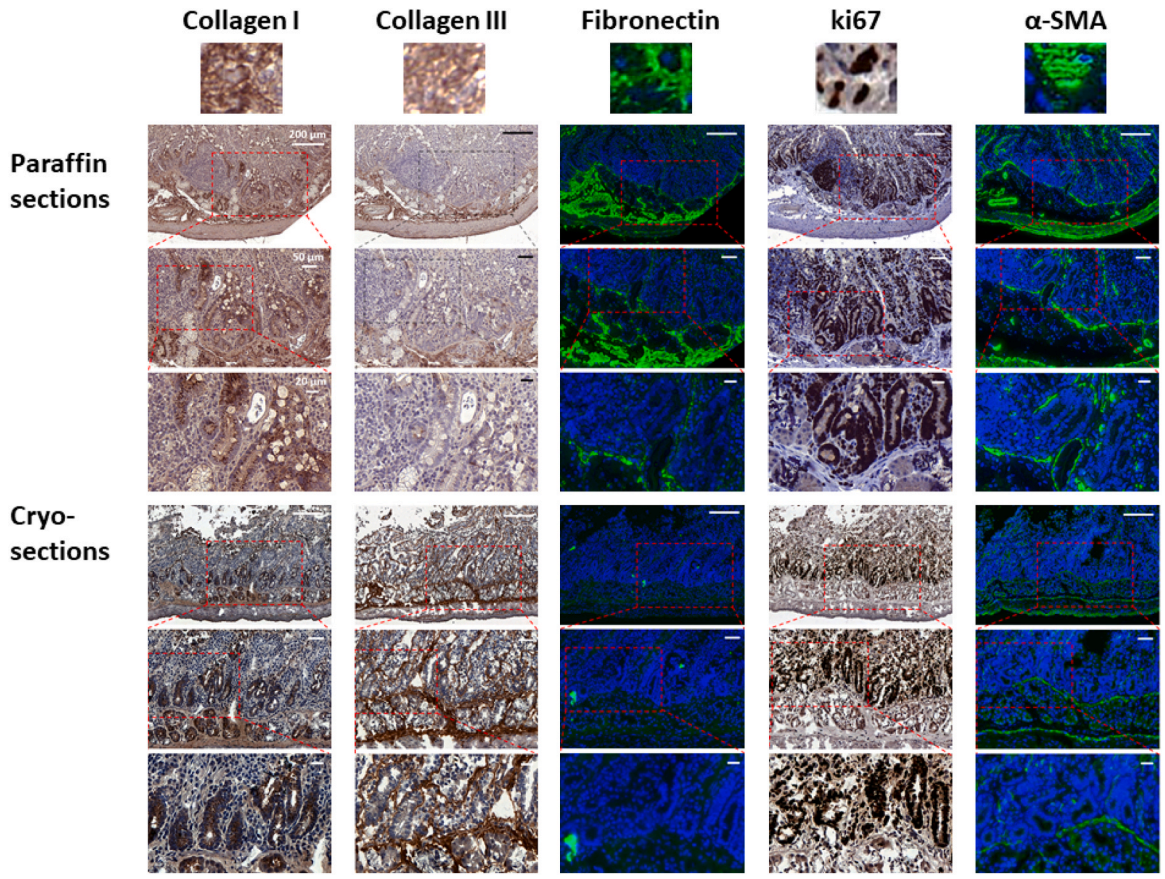

Fig. 1. Collagen I, collagen III, fibronectin, ki67 and α-SMA immunohistochemical labelling with DAB as chromogen (dark brown colour for collagen I, collagen III and ki67) and immunofluorescence detection (light green for fibronectin and α-SMA); with cell nuclei DAPI labelling, blue) for paraffin sections with antigen retrieval (AR, upper rows) and cryosections (lower rows). Corresponding inserts (dashed line) depict the area used for images at the next lower level.

the duodenum were slightly collagen III positive in paraffin sections (Fig. 1). However, in the cryosections, the collagen III intensity at these locations was much more pronounced. In addition to the serous membrane and the connective tissue, the lamina *muscularis mucosae* exhibited a clear collagen III positive staining in the cryosections, which was however sparsely visible in the paraffin sections.

While the duodenum tissue immunohistochemically stained for fibronectin exhibited clear green areas in the paraffin sections, the cryosections do not show such areas or are only very weak and slurry, resembling rather artefacts than real structures (Fig. 1). The superiority of the paraffin sections is clear: they have a much higher green-to-black contrast and the connective tissue between the glands is clearly visible. The fibronectin-positive areas are shown as fine lines at low magnification, better visible at higher magnifications and particularly found around the glands – coexistent with collagen I (Fig. 1).

The proliferation status of cells with the dark brown, practically black, ki67 positive cell nuclei in the connective tissue, were clearly and well visible for both paraffin and cryosections. Due to stronger brownish background staining found in the cryosections as compared to blueish background in paraffin sections, the paraffin sections had nevertheless to be favoured when the chromogenic DAB detection system was used. We found proliferative cells in the gland walls for practically all cells facing the lumen, however only in all glands that were not attributed to be Brunner's glands. While it has been reported for piglet duodenum that ki67 positive proliferative cells were found for $> 90\%$ in the surface epithelium, they were reported to be very low with $< 10\%$ in the Brunner's glands (Zhang et al., 2023), confirming our findings.

Moreover, the comparison of α-SMA staining with a fluorescent detection system (Fig. 1) revealed more pronounced staining intensities of green colour in paraffin sections than cryosections. Therefore, paraffin sections have to be favoured over cryosections, but also because the α-SMA positive areas in vessel walls of arteries and veins are a bit less slurry than in the corresponding cryosections. In the duodenum, the outer margin of the glands were stained all clearly α-SMA positive. In addition, the circular muscle with the serous membrane exhibited α-SMA positive areas.

Table 3 gives an overview of the recommendations to use either formalin fixation or cryo embedding for the previously discussed antibodies of Fig. 1.

3.2. Antigen retrieval (AR) for paraffin sections

In order to counteract the harmful effects of formalin treatment, antigen retrieval (AR) is optional, but in many cases a necessary step to overcome the compromised immunoreactivity of the antigens in paraffin

Table 3
Recommendations which technique is favoured for which purpose.

Antibody	*Detection system*	*Recommendation*
Collagen I	Chromogenic	Paraffin sections that have less background staining.
Collagen III	Chromogenic	Cryosections: distinction of collagen III positive areas easier (higher contrast).
Ki67	Chromogenic	Paraffin sections favoured over cryosections, because of stronger background staining in cryosections.
Fibronectin	Fluorescent	Paraffin sections favoured due to higher green-to-black contrast.
α-SMA	Fluorescent	Paraffin sections because of lower slurryness and better confinement of α-SMA positive areas.

embedded sections (Ramos-Vara, 2005). Analysis of protein localization within fixed samples can be complicated by crosslinks formed between proteins during formalin fixation which mask target epitopes. AR is introduced to reverse such crosslinks and improve the sensitivity of antibody-based protein detection (Dunkenberger and Del Valle, 2022). AR can be realized as heating the sections to approximately 100 °C in a microwave oven (Shi et al., 1991) or in steamers and pressure cookers (Ramos-Vara, 2017). AR is not restricted to crosslinking fixatives like formalin, but has been adapted to other fixation techniques like PAXgene tissue fixation (Stumptner et al., 2019). The buffers with specific pH values and the exact time frames for microwave processing have to be evaluated for each tissue, fixative and antibody under view (Stumptner et al., 2019).

After an AR step, tissue proteomics can be applied, bridging classical and molecular histology. To realize tissue proteomics and enable not only the validation of specific immunohistochemical labelling but also a more in-depth analysis of components, a matrix assisted laser desorption/ionization (MALDI) mass spectrometer can be used, which allows for differential mapping of hundreds of compounds at a distinct location of a section to further analyse the tissue (Longuespée et al., 2014).

To visualize the hugely positive effect of an AR step before immunohistochemical staining in paraffin sections, we present fibronectin and isotype negative control labelled sections with or without AR (Fig. 2). As can be seen in the fluorescent detection system, fibronectin positive duodenal tissue was only distinguishable (green) with an AR step (Fig. 2A), while the sections without AR were just black (no apparent signal) (Fig. 2B). Accordingly, some weak signals (mainly from erythrocytes) were seen in the Isotype negative control with AR, while again no signal was detectable without AR.

3.3. Chromogenic staining versus fluorescent detection system

For collagen I, collagen III, fibronectin, α-SMA and ki67 immunohistochemical labelling, we have compared chromogenic DAB/brightfield imaging with fluorescent detection system in paraffin sections with AR in serial sections (Fig. 3). While the extracellular markers collagen I and collagen III exhibited the glands of the rabbit duodenum better with DAB staining than the corresponding fluorescent detections system, for fibronectin and α-SMA, the distinct structures were slightly better visible (with more contrast) in the fluorescent detection system (Fig. 3A). We also compared ki67 labelling: in the chromogenic staining, the dark brown cell nuclei of the proliferating cells were very well visible, embedded in the connective tissue between the excretory ducts (Fig. 3B), while in the corresponding fluorescent detections system, the proliferating cells were visible, however, all the surrounding tissue was ki67 negative and therefore quite dark. Nevertheless, both, DAB and fluorescent detection clearly delineated the proliferating gland cells surrounding the lumen.

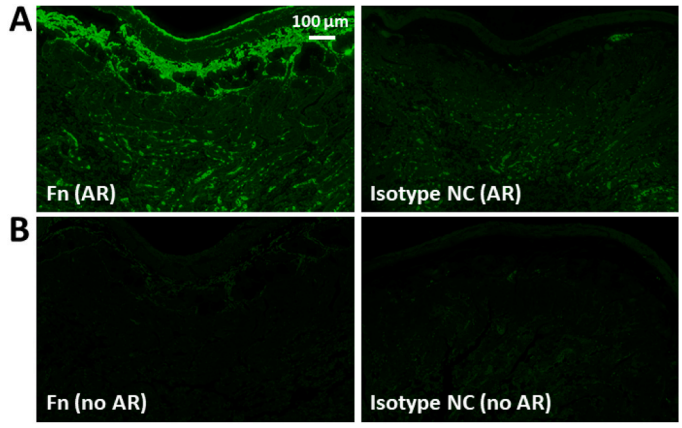

Fig. 2. Comparison of fibronectin and Isotype negative controls in paraffin sections with immunofluorescence (A and B) and with antigen retrieval (AR; A) or without AR (no AR; B) for duodenum tissue.

As optical colour loss is a general problem in immunofluorescence compared with the stable DAB chromogenic system, DAB is recommended rather than fluorescence in case there are no pronounced advantages of fluorescent labelling. Additionally, it has to be noticed that during slide scanning with digital microscopic devices, all slides have to be treated adequately in order to achieve full information with respect to the immunohistochemical labelling of target structures.

3.4. Anatomy of the rabbit duodenum

The rabbit duodenum including the serous membrane around the circular and longitudinal muscles is furthermore shown in detail in a HE stained section (Fig. 4A), where the intestinal glands with crypts, the villi, the arteries can be nicely seen besides the Brunner's glands, the lamina *muscularis mucosae* and the connective tissue in between.

Furthermore, we present similar excerpts with PAR-2 and ki67 immunolabelling (Fig. 4B). Interestingly, PAR-2 intensity is pronounced in the glands that are embedded in the connective tissue adjacent to the circular muscle tissue, but not in the intestinal glands nor in the Brunner's glands. In the PAR-2 positive glands, however, ki67 is only weakly expressed – which stands in contrast to the intestinal glands and the Brunner's glands that both show highly proliferating cells in the gland wall, particularly facing the lumen. The duodenum is exposed to proteases coming either from the gut or from the mucosa, including the host's digestive enzymes and the proteases released by microbiota. Active proteases are capable to translocate into the intestinal epithelium, particularly under inflammatory conditions. Therefore PAR-2 that is expressed throughout the gastrointestinal tract has been reported to impact gut permeability regulation, a major factor affecting intestinal physiology and metabolic inflammation (Pontarollo et al., 2020). Different PAR-2 expression levels have been associated with visceral hypersensitivity as studied in a rat model (Zhao et al., 2022).

Furthermore, we provide more detailed images of Brunner's glands, intestinal glands, lymph nodes and duodenal arteries and veins, with collagen I, collagen III, fibronectin, α-SMA, PAR-2, HE, GT (Masson Goldner Trichrome) and EL (Elastica von Gieson) for elastin stainings (Fig. 5). The Brunner's glands exhibited particularly weak collagen I and collagen III staining, which is confirmed in the fluorescently labelled sections, where there is practically no green intensity (Fig. 5A). Moreover, neither fibronectin, α-SMA nor ki67 positive cells can be distinguished. In contrast to another type of glands situated next to Brunner's glands also visible in Fig. 5A, the Brunner's glands that secrete cholecystokinin and secretin, do not express PAR-2 protein. In the PAR-2 positive glands, the role of PAR-2 may be associated with the direct regulation of the glandular exocrine secretion, as reported for PAR-2 positive cells in rat and murine glands (Kawabata et al., 2000).

As for the intestinal glands, they are collagen I ositive, however, collagen III negative and show some weak fibronectin staining (Fig. 5B). Most prominent is the high abundance of ki67 positive cells in the wall of the intestinal glands. While elastin was completely absent in the Brunner's glands (Fig. 5A), some elastin is associated with structures representing the intestinal glands (Fig. 5B). Finally, PAR-2 staining can be seen, but it is not very strong, particularly weaker than in the glands adjacent to the Brunner's glands (Fig. 5A).

Serial sections of lymph nodes in the duodenum are shown in Fig. 5C. While lymph nodes in the liver were PAR-2 negative (Meier-Bürgisser et al., 2021), lymph nodes in the duodenum showed few PAR-2 positive areas. Striking was the high fraction of ki67 positive cells in the lymph node, accompanied by an extracellular matrix dominated by collagen I and fibronectin, but few collagen III and no α-SMA.

In the walls of arteria and veins, there was practically no collagen I and III, however, fibronectin and more so α-SMA were the predominating extracellular matrix components (Fig. 5D). Only few proliferating and ki67 positive cells were found. And PAR-2 staining was

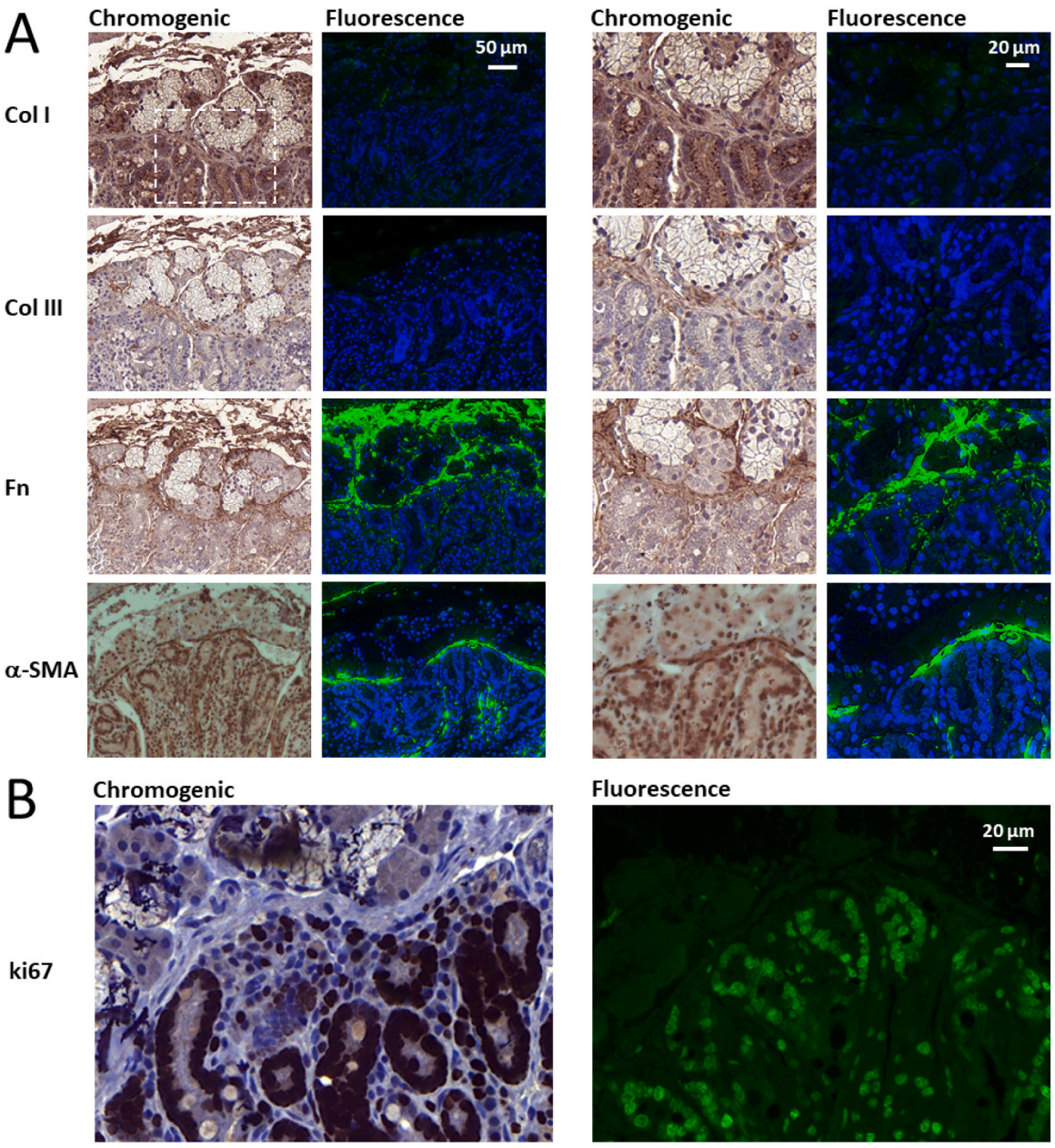

Fig. 3. Immunohistochemical labelling for collagen I, collagen III, fibronectin, α-SMA (A) and ki67 (B) in duodenum tissue, for chromogenic staining with subsequent bright field imaging (left; DAB as chromogen) and immunofluorescence staining and imaging (right) for two magnifications (squares with white dashed line in the first image represents the zone at higher magnification on the right side). All samples were paraffin embedded and labellings performed with AR.

particularly pronounced in the lumen of the arteries, very similar as found for the glands situated adjacent to the Brunner's glands.

In Fig. 6, cryo sections of the Brunner's glands and the intestinal glands are presented. The labellings for collagen I and collagen III resulted in good images and the corresponding structures can be delineated well. In contrast, fibronectin labelled cryo sections were rather poor compared to corresponding fluorescent paraffin sections (Fig. 5A) because the immunohistochemically provoked green intensity was slurry and not as distinct as in the paraffin version. For α-SMA labelling as well as the ki67 and its negative control, good and very well visible structures and proliferating cells, respectively, were obtained also in cryosections (Fig. 6).

Finally, we present an overview of different HE stained sections from the gastrointestinal tract (Fig. 7). Starting in the rabbit stomach, we present images of the duodenum, the small intestine (several portions), the large intestine (several portions) and the rectum. As can be seen, the transitions between the different organs are anatomically graded. For example, the transition from the duodenum to the small intestine is reflected in the initial part of the small intestine with very similar anatomical composition as observed for the duodenum. Only in the second part of the small intestine the change towards a more pronounced gland-rich area is delineated. Moreover, the circular muscle of the large intestine is larger than in the small intestine and the duodenum, while in the rectum, it is approximately of the same thickness as in the duodenum (Fig. 7).

3.5. *Conclusive remarks*

We have shown that histological staining for elastin, haematoxylin&eosin, Masson Goldner Trichrome and immunohistochemical labelling for collagen I and III, α-SMA, fibronectin, ki67 and PAR-2 is feasible in the healthy rabbit duodenum tissue. The main structures

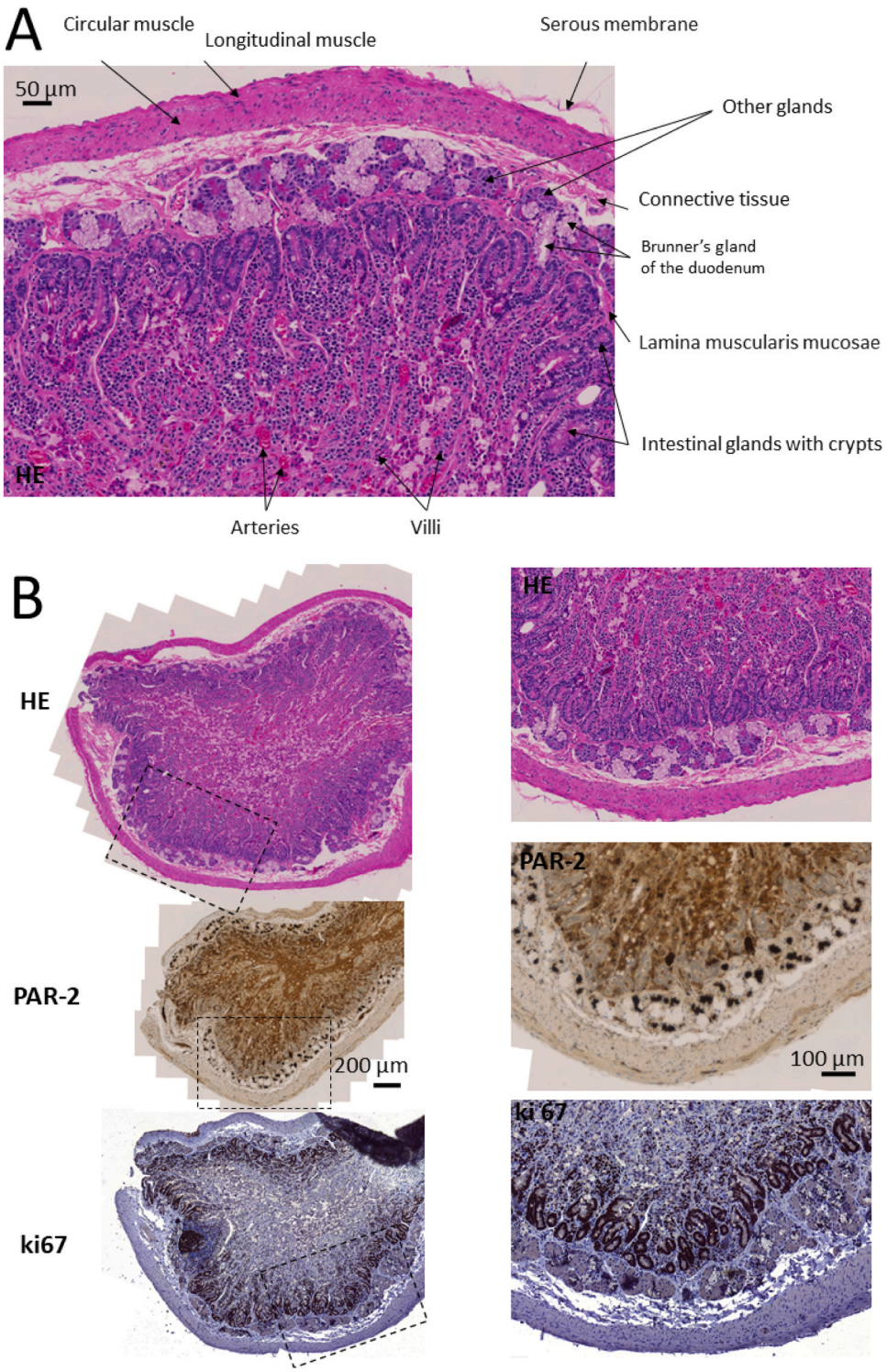

Fig. 4. Specific structures and tissue in a healthy rabbit duodenum section. Overview (HE staining) (A), excerpts with HE, PAR-2 and ki67 stainings (B).

(intestinal glands, Brunner's glands, circular and longitudinal muscle tissue), can be depicted well. Recommendations are given on whether paraffin sections or cryosections may serve specific purposes better. Moreover, we show in a side-by-side comparison that an antigen retrieval step for formalin fixation and paraffin embedding is extremely valuable. Finally, as PAR-2 expression has not been described in the New Zealand white rabbit duodenum so far, we showed the PAR-2 distribution and found a predominant PAR-2 protein expression in the lumen of some arteries and in the glands very near to the Brunner's glands, but not in the Brunner's glands themselves.

Several limitations have to be addressed. We only deal with the healthy state of the duodenum and not the diseased or inflamed state because this would be beyond the scope of a technical note that focuses on the juxtaposition of different stainings. In addition, we have dealt with the gastrointestinal tract of only one rabbit – and therefore are not able to elucidate potential inter-rabbit variability. However, as New Zealand white rabbits have all the same genetic background, we judge the anatomy of the healthy rabbit to be very similar and coherent over

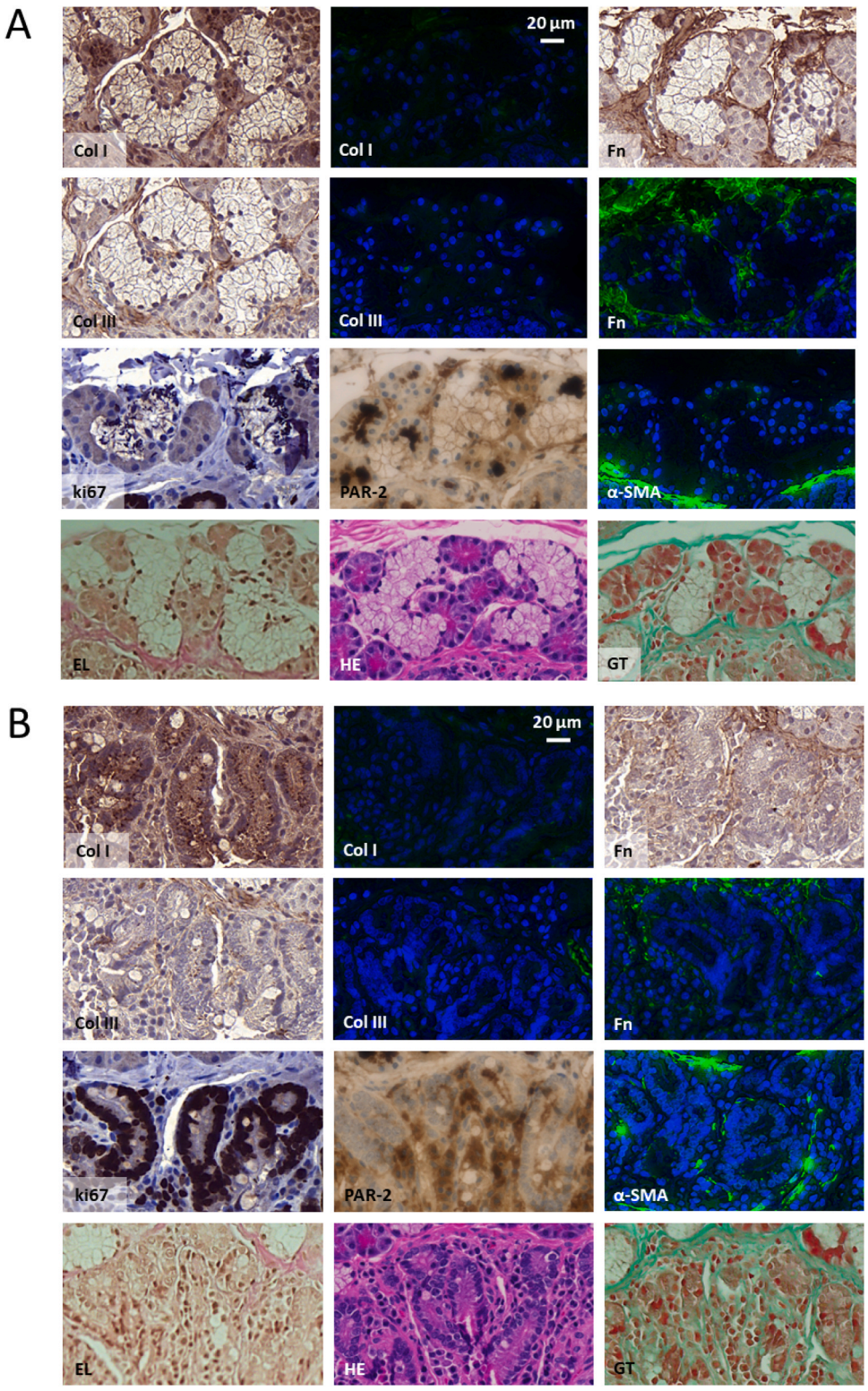

Fig. 5. Different structures in the rabbit duodenum immunohistochemically labelled for a series of different markers as well as HE and EL (in paraffin sections with AR). Brunner's glands (A), intestinal glands (B), lymph nodes (C) and arteria and veins (D): *Key*: HE = Haematoxylin&Eosin, Fn = Fibronectin, α-SMA = alpha smooth muscle actin, PAR-2 = protease activated receptor-2, EL = Elastica van Gieson staining for elastin.

many New Zealand white rabbits.

To conclude, histological and immunohistochemically stained sections of the healthy rabbit duodenum are presented to be used for a comparison with the pathological situation when visceral researchers have decided to use this animal model.

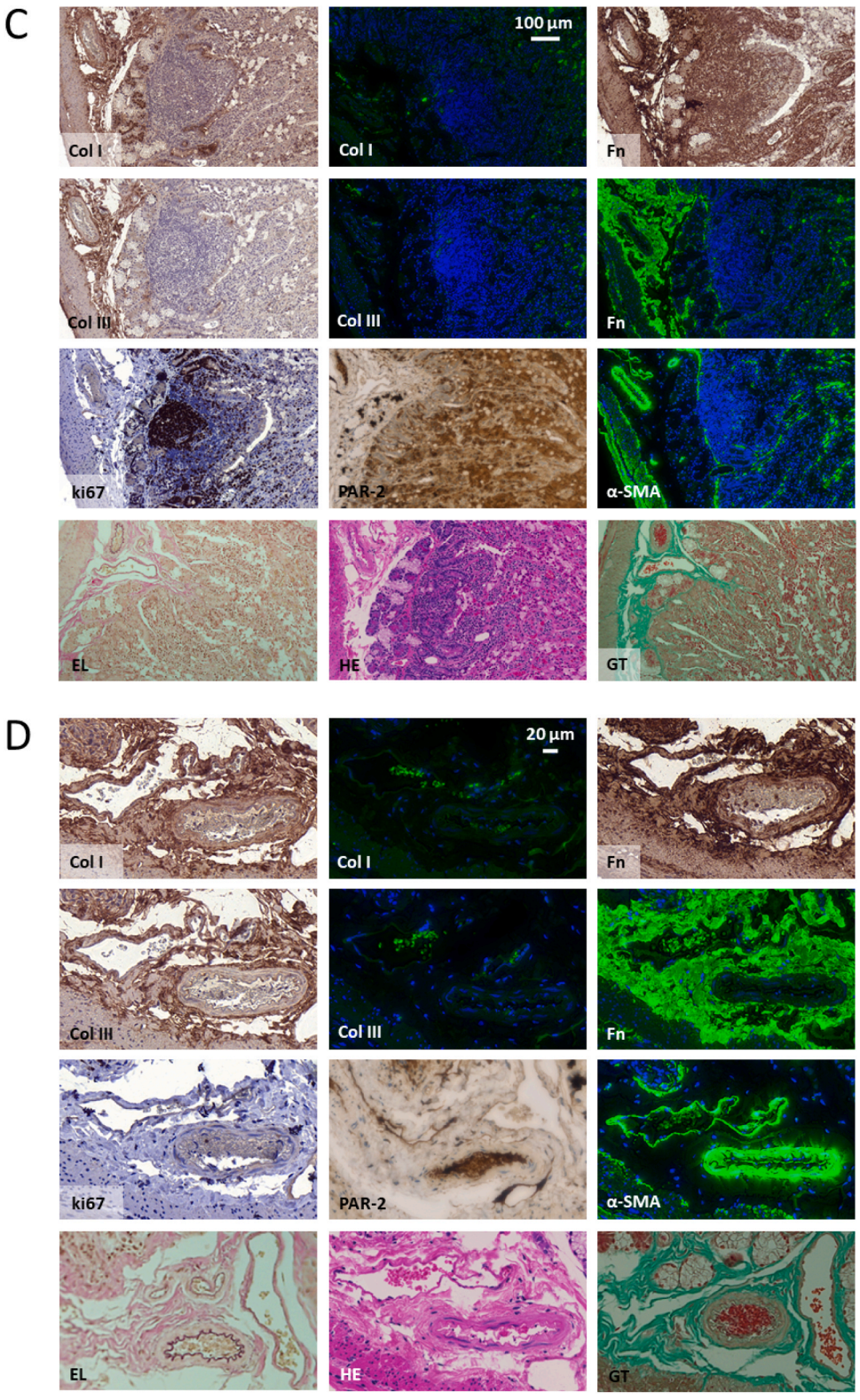

Fig. 5. (*continued*).

CRediT authorship contribution statement

Buschmann Johanna: Writing – review & editing, Writing – original draft, Validation, Supervision, Resources, Project administration, Conceptualization. **Calcagni Maurizio:** Writing – review & editing, Supervision. **Giovanoli Pietro:** Writing – review & editing, Supervision. **Heuberger Dorothea M.:** Validation, Supervision, Methodology. **Meier Bürgisser Gabriella:** Writing – original draft, Methodology, Investigation, Formal analysis, Data curation, Conceptualization.

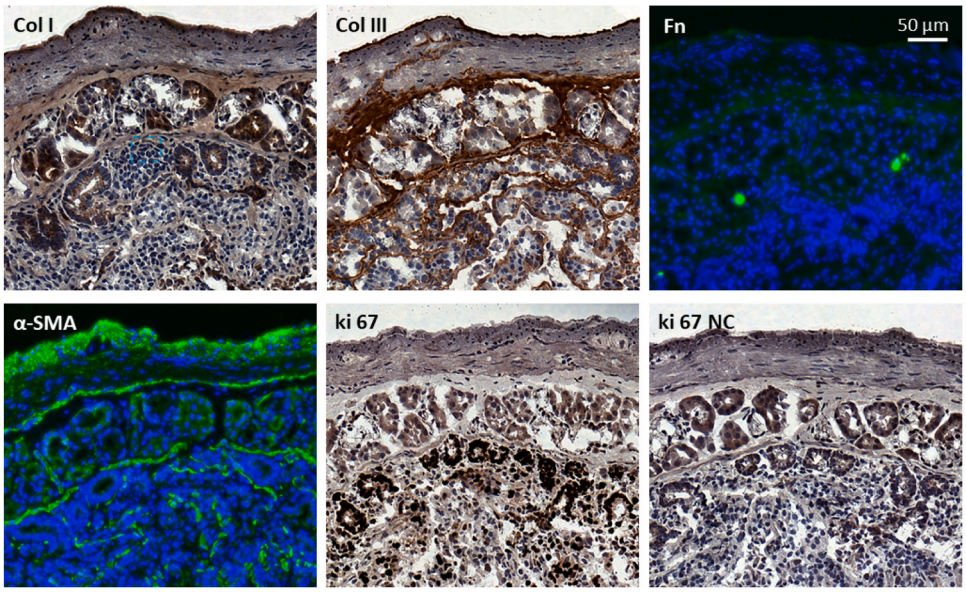

Fig. 6. Brunner's and intestinal gland in cryo ssections of healthy rabbit duodenum tissue stained with collagen I, collagen III, fibronectin, α-SMA, ki67, and negative control for ki67, respectively *Key*: Col = Collagen, Fn = Fibronectin, α-SMA = alpha smooth muscle actin, ki67 = proliferation marker ki67.

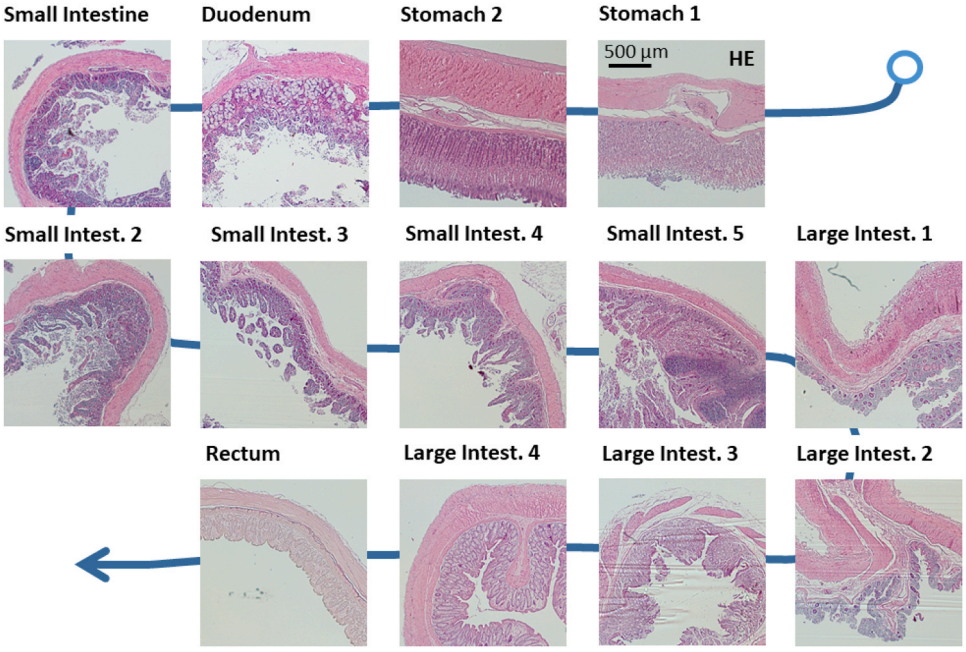

Fig. 7. Digestive tract, HE staining, showing the different portions of the stomach, the small intestine, the large intestine and the rectum, respectively. *Key*: Intest. = Intestine.

Declaration of Competing Interest

The authors declare that they have no known competing financial interests or personal relationships that could have appeared to influence the work reported in this paper.

Data availability

Data will be made available on request.

Acknowledgements

Olivera Evrova is highly acknowledged for establishment of IHC stainings (except for PAR-2) and for her comments on the manuscript. We thank Flora Nicholls for extraction of the whole gastrointestinal tract from the cadaver rabbit. Prof. Reto A. Schüpbach is kindly acknowledged for his input during discussions. Furthermore, we thank Ines Kleiber-Schaaf and Andrea Garcete-Bärtschi for their help with tissue sections and HE, GT and EL stainings. We thank Silvia Behnke from Sophistolab, Switzerland, for PAR-2 immunohistochemical staining. The center for microscopy (ZMB) at University of Zurich and the Scope M at ETH Zurich are highly acknowledged for scanning the histological slides.

Author contributions

GMB performed IHC stainings (except for PAR-2), imaged all sections and composed all figures. DMH gave valuable input on PAR-2 staining. MC, PG and JB supervised the study. JB provided funding, wrote the manuscript and supervised the study.

References

Amiry, A.F., Kigata, T., Shibata, H., 2019. Wall thickness and mucous cell distribution in the rabbit large intestine. J. Vet. Med. Sci. 81 (7), 990–999.

Dunkenberger, L., Del Valle, L., 2022. Antigen retrieval and signal amplification. Methods Mol. Biol. 242265–242274.

Flemström, G., Garner, A., 1984. Some characteristics of duodenal epithelium. Ciba Found. Symp. 10994. -108.

Fowler, C.B., O'Leary, T.J., Mason, J.T., 2008. Modeling formalin fixation and histological processing with ribonuclease A: effects of ethanol dehydration on reversal of formaldehyde cross-links. Lab. Invest. 88 (7), 785–791.

Ghayor, C., Weber, F.E., 2018. Osteoconductive microarchitecture of bone substitutes for bone regeneration revisited. Front. Physiol. 9960..

Hira, V.V.V., de Jong, A.L., Ferro, K., Khurshed, M., Molenaar, R.J., Van Noorden, C.J.F., 2019. Comparison of different methodologies and cryostat versus paraffin sections for chromogenic immunohistochemistry. Acta Histochem 121 (2), 125–134.

Hou, C., Zhang, H., Wang, X., Yang, Z., 2022. The "Hand as Foot" teaching method in the duodenum anatomy. Asian J. Surg. 45 (9), 1768–1769.

Johansson, M.E., Sjövall, H., Hansson, G.C., 2013. The gastrointestinal mucus system in health and disease. Nat. Rev. Gastroenterol. Hepatol. 10 (6), 352–361.

Katoh, M., 2017. Canonical and non-canonical WNT signaling in cancer stem cells and their niches: cellular heterogeneity, omics reprogramming, targeted therapy and tumor plasticity (Review). Int. J. Oncol. 51 (5), 1357–1369.

Kawabata, A., Nishikawa, H., Kuroda, R., Kawai, K., Hollenberg, M.D., 2000. Proteinase-activated receptor-2 (PAR-2): regulation of salivary and pancreatic exocrine secretion in vivo in rats and mice. Br. J. Pharmacol. 129 (8), 1808–1814.

Kawabata, A., Kinoshita, M., Nishikawa, H., Kuroda, R., Nishida, M., Araki, H., Arizono, N., Oda, Y., Kakehi, K., 2001. The protease-activated receptor-2 agonist induces gastric mucus secretion and mucosal cytoprotection. J. Clin. Invest. 107 (11), 1443–1450.

Kimmins, M.H., Billingham, R.P., 2001. Duodenal Crohn's disease. Tech. Coloproctol. 5 (1), 9–12.

Krause, W.J., 2000. Brunner's glands: a structural, histochemical and pathological profile. Prog. Histochem. Cytochem. 35 (4), 259–367.

Longuespée, R., Fléron, M., Pottier, C., Quesada-Calvo, F., Meuwis, M.A., Baiwir, D., Smargiasso, N., Mazzucchelli, G., De Pauw-Gillet, M.C., Delvenne, P., De Pauw, E., 2014. Tissue proteomics for the next decade? Towards a molecular dimension in histology. OMICS 18 (9), 539–552.

Meier Bürgisser, G., Evrova, O., Heuberger, D.M., Calcagni, M., Giovanoli, P., Buschmann, J., 2020. Delineation of the healthy rabbit lung by immunohistochemistry – a technical note. Acta Histochem, 151648.

Meier Bürgisser, G., Heuberger, D.M., Giovanoli, P., Calcagni, M., Buschmann, J., 2021. Delineation of the healthy rabbit kidney by immunohistochemistry – A technical note. Acta Histochem 123 (4), 151701.

Meier Bürgisser, G., Heuberger, D.M., Schaffner, N., Giovanoli, P., Calcagni, M., Buschmann, J., 2022. Delineation of the healthy rabbit heart by immunohistochemistry - A technical note. Acta Histochem 125 (1), 151993.

Meier-Bürgisser, G., Evrova, O., Heuberger, D.M., Rieber, J., Giovanoli, P., Calcagni, M., Buschmann, J., 2021. Delineation of the healthy rabbit liver by immunohistochemistry – A technical note. Acta Histochem 123 (7), 151795.

Pontarollo, G., Mann, A., Brandão, I., Malinarich, F., Schöpf, M., Reinhardt, C., 2020. Protease-activated receptor signaling in intestinal permeability regulation. FEBS J. 287 (4), 645–658.

Prentø, P., Lyon, H., 1997. Commercial formalin substitutes for histopathology. Biotech. Histochem. 72 (5), 273–282.

Ramos-Vara, J.A., 2005. Technical aspects of immunohistochemistry. Vet. Pathol. 42 (4), 405–426.

Ramos-Vara, J.A., 2017. Principles and methods of immunohistochemistry. Methods Mol. Biol. 1641115–1641128.

Rosas-Arellano, A., Villalobos-González, J.B., Palma-Tirado, L., Beltrán, F.A., Cárabez-Trejo, A., Missirlis, F., Castro, M.A., 2016. A simple solution for antibody signal enhancement in immunofluorescence and triple immunogold assays. Histochem. Cell Biol. 146 (4), 421–430.

Ryska, A., Sapino, A., Landolfi, S., Valero, I.S., Cajal, S.R.Y., Oliveira, P., Detillo, P., Lianas, L., Frexia, F., Nicolosi, P.A., Monti, T., Bussolati, B., Marchiò, C., Bussolati, G., 2023. Glyoxal acid-free (GAF) histological fixative is a suitable alternative to formalin: results from an open-label comparative non-inferiority study. Virchows Arch.

Sadeghipour, A., Babaheidarian, P., 2019. Making formalin-fixed, paraffin embedded blocks. Methods Mol. Biol. 1897253–1897268.

Salguero, F.J., Mekonnen, T., Ruiz-Villamor, E., Sanchez-Cordon, P.J., Gomez-Villamandos, J.C., 2001. Detection of monokines in paraffin-embedded tissues of pigs using polyclonal antibodies. Vet. Res. 32 (6), 601–609.

Seman, M., Kasereka-Kisenge, F., Taieb, A., Noullet, S., Trésallet, C., 2019. Resection of the third and four portions of the duodenum. J. Visc. Surg. 156 (1), 45–49.

Shi, S.R., Key, M.E., Kalra, K.L., 1991. Antigen retrieval in formalin-fixed, paraffin-embedded tissues: an enhancement method for immunohistochemical staining based on microwave oven heating of tissue sections. J. Histochem. Cytochem. 39 (6), 741–748.

Siegenthaler, B., Ghayor, C., Ruangsawasdi, N., Weber, F.E., 2020. The release of the bromodomain ligand N,N-Dimethylacetamide adds bioactivity to a resorbable guided bone regeneration membrane in a rabbit calvarial defect model. Materials 13 (3), 501.

Stumptner, C., Pabst, D., Loibner, M., Viertler, C., Zatloukal, K., 2019. The impact of crosslinking and non-crosslinking fixatives on antigen retrieval and immunohistochemistry. N. Biotechnol. 5269–5283.

Takahashi, H., Yao, K., Nagahama, T., Miyaoka, M., Ohtsu, K., Kanemitsu, T., Matsunaga, K., Ueo, T., Ueki, T., 2022. Visualization of absorbed lipid in the normal duodenal epithelium using magnifying endoscopy with narrow-band imaging. Dig. Dis. Sci. 67 (12), 5610–5616.

Tsutsumi, Y., 2021. Pitfalls and caveats in applying chromogenic immunostaining to histopathological diagnosis. Cells 10 (6).

Yu, G., Xu, S., Kong, J., He, J., Liu, J., 2023. Development and validation of web calculators to predict early recurrence and long-term survival in patients with duodenal papilla carcinoma after pancreaticoduodenectomy. BMC Cancer 23 (1), 1129.

Zhang, W., Wang, X., Lanzoni, G., Wauthier, E., Simpson, S., Ezzell, J.A., Allen, A., Suitt, C., Krolik, J., Jhirad, A., Dominguez-Bendala, J., Cardinale, V., Alvaro, D., Overi, D., Gaudio, E., Sethupathy, P., Carpino, G., Adin, C., Piedrahita, J.A., Mathews, K., He, Z., Reid, L.M., 2023. A postnatal network of co-hepato/pancreatic stem/progenitors in the biliary trees of pigs and humans. NPJ Regen. Med 8 (1), 40.

Zhao, L., Ren, P., Wang, M., Wang, J., He, X., Gu, J., Lu, Y., Wu, Y., Liu, J., Wang, L., Li, H., 2022. Changes in intestinal barrier protein expression and intestinal flora in a rat model of visceral hypersensitivity. Neurogastroenterol. Motil. 34 (4), e14299.

Zheng, X.L., Kitamoto, Y., Sadler, J.E., 2009. Enteropeptidase, a type II transmembrane serine protease. Front. Biosci. 1 (1), 242–249.